

Hybrid Cooperative Reconnaissance Without Communication

Paul G. Otanez and Mark E. Campbell
Department of Mechanical and Aerospace Engineering
Cornell University
Ithaca, NY 14853
potanez@cornell.edu, mc288@cornell.edu

Abstract—The cooperative reconnaissance performance of two vehicles in an uncertain environment while minimizing communication is investigated. Instead of direct communication, information between vehicles is transferred using mode perturbation signatures based on Gold codes. The behavior of the observed vehicle is modelled as a hybrid system with a finite number of operating modes defined by the vehicle's dynamics and a perturbation signature. The second vehicle estimates the operating mode of the first vehicle in order to collaborate in collecting information. The performance of the system is gauged using two metrics: 1) by the length of time required for the two vehicles to collect a certain level of information, and 2) by the amount of information collected in a time interval. The follower decides whether cooperation is advantageous by evaluating one of the performance metrics. Monte Carlo simulations of the system are compared to a decentralized system in which there is no cooperation and a centralized system with full communication.

I. INTRODUCTION

Unmanned vehicles, such as robots, aerial and underwater vehicles, have been identified as attractive solutions in civilian and military applications where the environment is too dangerous and/or too expensive to use a human operator. The advantages of unmanned vehicles are well documented and include: significant weight savings, low risk for human operators, and potential for superior coordination [1]. "Swarms" of smaller versions of these vehicles are now being envisioned because of the advantages of building small scale electronics and integrate the smart sensor and software technologies on board, economies of scale, and robustness. However, creating and maintaining a communication network (intra-vehicle) would be excessively complicated and not scale well with the numbers of vehicles. The work here defines a strict constraint on communication and focuses on the problem of cooperative control with little communication.

Inherent to cooperative vehicles without communication is the need of each vehicle to estimate the behavior of its environment in order to improve its performance and decision making. The environment includes partner vehicles or adversarial vehicles whose behavior can be described by a finite number of operating modes. Because the behavior of the system is described by a finite set operating modes, the environment can be modelled using a hybrid automaton. A hybrid system can loosely be defined as a system in which there is an interaction of discrete (the operating modes) and continuous dynamics (the vehicle's state) [2]. An estimation/detection scheme must then determine the current operating mode of the hybrid system from measurements of the environment.

The problem of state (sometimes referred to as the base-state) and mode (sometimes referred to as the modal state) estimation in hybrid systems has been addressed in literature. The Interacting Multiple Model (IMM) estimator developed in [3] fuses N models to efficiently compute a high quality state estimate. Fusion is based on computing the probability of the modes based on their residuals; the mode with the smaller residual is weighted more in the estimate. For nonlinear systems that have unknown but

bounded uncertainties, a hybrid estimator is derived in [4]. Mode switching occurs based on a metric to minimize the uncertainty in the state estimate. The marginal performance of the Extended Kalman Filter (EKF) in certain tracking/recognition problems led to the development of the Polymorphic Estimator (PME). In contrast to the previously mentioned estimators, Ref. [5] proposes a moving-horizon estimation (MHE) algorithm for hybrid systems modelled in the mixed logic dynamical form. The implementation of MHE relies on solving a mixed-integer quadratic program that depends on initial penalties, which improve the estimate in the presence of noise. In [6], the authors propose defining each mode using the system dynamics as well as perturbation signatures. When these signatures are chosen such that they have favorable cross-correlation properties, the estimates can be correlated with the signatures, thus allowing mode detection.

This paper investigates the use of mode perturbation signatures to achieve cooperative reconnaissance without communication between two vehicles searching a random environment. The mode perturbation signatures developed in [6] are used to correlate Gold codes to the operating modes of a vehicle. A correlation test is then used to detect the mode of operation. The cooperative reconnaissance performance of the system using mode perturbation signatures is tested in two ways: 1) by measuring the length of time it takes for the vehicles to collect information from an area, and 2) by the amount of information collected in a fixed time interval. Section II describes the hybrid system model and summarizes mode perturbation signatures for estimation. In Section III, the cooperative reconnaissance environment is described. Finally, Section IV presents a Monte Carlo approach used to analyze the cooperative reconnaissance performance of the vehicles using perturbation signatures. The performance of the system is compared to a decentralized system in which there is no cooperation and a centralized system with full communication.

II. HYBRID MODEL AND MODE PERTURBATION SIGNATURES

A. Hybrid Model

It is assumed that the behavior of each vehicle can be described by a finite set of operating modes. Using a hybrid automaton, the system is described in a hybrid framework as shown in Figure 1. Each node, q_i , in the automaton corresponds to one of the N operating modes. The state evolution while inside a node is governed by the following equations:

$$\mathbf{x}(\mathbf{k}+1) = A^i \mathbf{x}(\mathbf{k}) + B^i \left[u(k) + u_{sig}^i(k) \right] \quad (1)$$

$$\mathbf{y}(\mathbf{k}) = C^i \mathbf{x}(\mathbf{k}) + D^i \left[u(k) + u_{sig}^i(k) \right] \quad (2)$$

where at time k , $\mathbf{x}(\mathbf{k})$ is the state, $\mathbf{y}(\mathbf{k})$ the measurement, $u(k)$ is the control input, and $u_{sig}^i(k)$ is a signature corresponding to the i^{th} mode. In contrast to most hybrid system formulations, the state

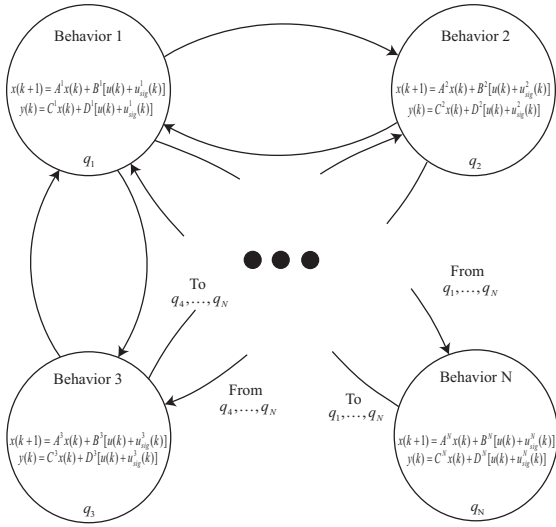


Fig. 1. Hybrid automaton with N nodes corresponding to the operating modes or behaviors.

evolution while inside a node i is not only influenced by the model (A^i, B^i, C^i, D^i), but also by an extra input u_{sig}^i . The relationship between each operating mode and its signature is explained next.

B. Mode Perturbation Signatures

The behavior of the observed vehicle can be fully described by N modes that are each correlated with a signature. The signature is a small perturbation, $u_{sig}^i(k)$, to the nominal control input of the observed vehicle, $u(k)$,

$$\underline{u}^i(k) = u(k) + u_{sig}^i(k), \quad (3)$$

where \underline{u}^i is the total control input of the observed vehicle. The nominal control input is the input necessary for the vehicle to perform its current task. The signatures, u_{sig}^i , must be small enough so that the vehicle is able to perform its current task, yet “large” enough to be able to propagate through the system dynamics and be detected (by an estimator) in the presence of process and measurement noise. Ideally the signatures are designed to be uncorrelated between themselves and unique to differentiate them from noise.

The mode perturbation signature, u_{sig} , is defined in a binary fashion and is composed of n bits. The selection of the modulation method to encode the signature into the signal is dependent on several factors that include: power requirements, required probability of detection, bandwidth efficiency, uncertainty in carrier phase reference, etc. One binary encoding method, referred to as amplitude-shift keying (ASK) in literature, consists in representing the 0 bit by a sequence, β^0 , of p points with value of zero while the 1 bit (on) is represented by a sequence, β^1 , of p points with a value determined by a sinusoid with amplitude δ and frequency ω ,

$$\beta^0 = [0, \dots, 0] \quad (4)$$

$$\beta^1 = [\delta \sin(\omega T j)] \quad (5)$$

for $j = \{1, \dots, p\}$ where T is the sampling time and $\beta^0, \beta^1 \in \mathbb{R}^p$. By combining n bits, a mode signature is defined. As an example, for a system encoded with ASK with three operating modes, $N = 3$,

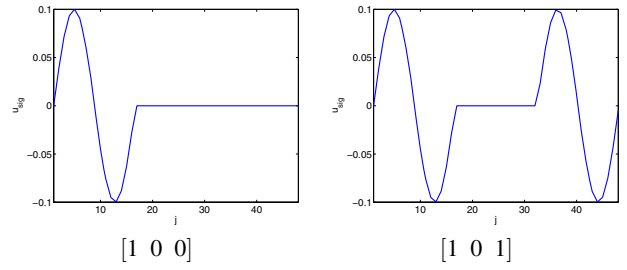


Fig. 2. Possible mode signatures for a system with three modes using ASK.

the corresponding mode signatures with $\delta = 0.1$ and $\omega = 30$ rad/sec are shown in Figure 2.

Consider a second binary encoding method:

$$x_m(t) = c(t) \cos(\omega_c t + \phi_0), \quad (6)$$

where $x_m(t)$ is the modulated signal, $c(t)$ is the signature, ω_c is the carrier frequency, and ϕ_0 carrier phase uncertainty. If the signature takes on values of ± 1 , then $c(t)$ modulates the signal by phase shifting the carrier by π radians. This signaling scheme is referred to as binary-shift keying (BPSK) and is used in various applications including GPS. Both ASK based BPSK based signature formulations scale well because more bits can be added as the number of modes increases.

Pseudorandom noise (PRN) is a known sequence of bits that, when added to a base signal, results in a signal that has statistical properties similar to noise [7]. An observer could recover the base signal only through correlation with a known sequence which is the exact replica of the original PRN. Certain PRN sequences, which include the Gold codes, have desirable properties in terms of cross-correlation. The cross-correlation function for two binary sequences d and e is defined as follows:

$$R_c(\tau) = \frac{1}{T} \int_0^T d(t)e(t+\tau)dt, \quad (7)$$

where T is the period of the sequences and τ is a delay. One advantage of Gold codes is that the cross-correlation or auto-correlation ($e = d$) function takes on three known values. Applying Equation (7) to two sequences determines whether two signals are correlated and if there exists a delay between the signals. Because of the favorable cross-correlation properties, Gold codes are used in Code Division Multiple Access (CDMA), and to define the mode signatures in this paper [8].

Because u_{sig} is defined using the observed vehicle internal time clock, the estimator must determine its clock offset, τ , in order to synchronize the expected signature, \tilde{u}_{sig} . This problem is also encountered in (GPS) where the signal traveling time is determined by the time shift required for a match between the received code from the satellite and the receiver replica [9]. To determine the clock offset, a correlation test (similar to Equation (7)) is performed on u_{sig} and the expected signature time shifted by the clock offset, $\tilde{u}_{sig}(\tau)$. The correlation test consists of computing the dot product of $u_{sig}(t)$ and the expected signature shifted by the clock offset $\tilde{u}_{sig}(t + \tau)$,

$$S(\tau) = \frac{1}{T} \int_0^T u_{sig}(t)\tilde{u}_{sig}(t + \tau)dt. \quad (8)$$

To find the delay, τ is varied over a range, Γ , from 0 to twice the period, $\Gamma \in [0, \dots, 2T]$. It is assumed in this work that each cell, $\tau(m) = m\frac{2T}{k}$ for $m \in \{0, \dots, k-1\}$, is equally probable of being the correct delay. Under the assumption of the absence of noise,

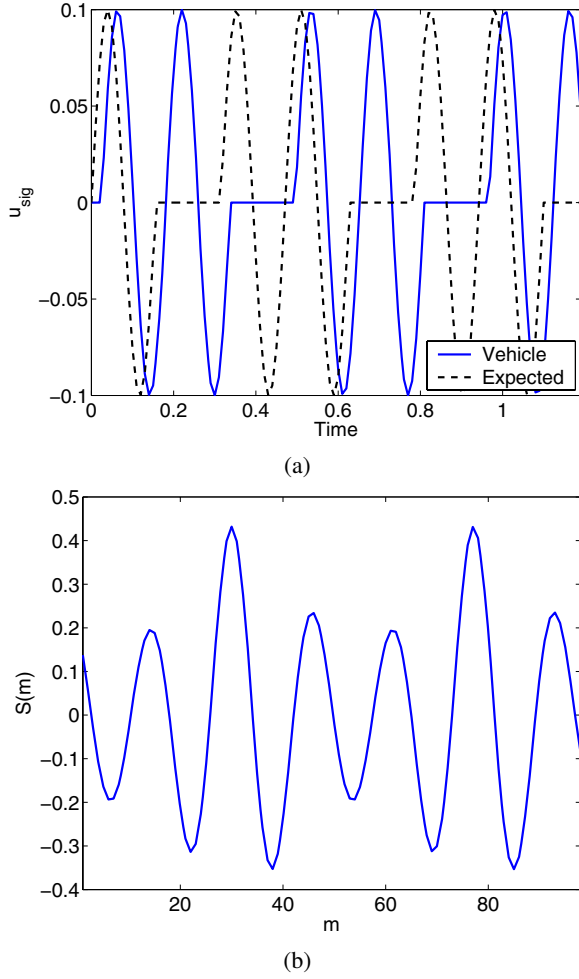


Fig. 3. The clock offset between the vehicle and expected signature and the time shift correlation.

the value of m that maximizes S , Equation (8), is the clock offset or delay. To illustrate the concept of a correlation test, Figure 3(a) shows that the vehicle and the expected signatures are not in phase. Figure 3(b) shows a plot of S as a function of m . Since the maximum value of S is found at $m = 30$, the clock offset can be computed.

C. Mode Estimation Methods

The purpose of correlating a signature u_{sig}^i with each of the nodes q_i is to facilitate mode estimation. By knowing which mode a partner vehicle is in, a higher quality of cooperation can be achieved. In this section, three mode estimation schemes are presented. Unless otherwise noted, the term “estimator” refers to any of the following estimators: the Kalman Filter for linear systems, the extended Kalman Filter and the Sigma Point Filter for nonlinear systems.

1) *Behavioral Mode Estimator*: The behavioral estimator estimates the state, $\hat{\mathbf{x}}$, from measurements and then correlates $\hat{\mathbf{x}}$ with the idealized behavior of the vehicle, $\tilde{\mathbf{x}}^i$, for each of the N modes. The idealized behavior is computed using the model for each of the modes with its corresponding signature,

$$\tilde{\mathbf{x}}^i(\mathbf{k}+1) = F^i \tilde{\mathbf{x}}^i(\mathbf{k}) + G^i \tilde{u}^i, \quad (9)$$

where $\tilde{u}^i = \tilde{u} + \tilde{u}_{sig}^i$ for $i \in \{1, \dots, N\}$. Over a horizon of H steps, the estimator computes the error between $\hat{\mathbf{x}}$ and $\tilde{\mathbf{x}}^i$,

$$\mathbf{v}^i(\mathbf{k}) = \begin{bmatrix} \hat{\mathbf{x}}(\mathbf{k}) - \tilde{\mathbf{x}}^i(\mathbf{k}) \\ \vdots \\ \hat{\mathbf{x}}(\mathbf{k}-H) - \tilde{\mathbf{x}}^i(\mathbf{k}-H) \end{bmatrix}. \quad (10)$$

The vector \mathbf{v}^i is a good measure of “goodness” of a mode match. There are several options to reduce this measure into a single metric that include: 1) the 1-norm of the residuals for each of the modes, 2) testing that the residuals are zero mean, and 3) and relying on a correlation test between $\hat{\mathbf{x}}(\mathbf{k})$ and $\tilde{\mathbf{x}}^i(\mathbf{k})$.

2) *Filter Based Mode Estimator*: A filter based mode estimator can be used when the control input, u , is unknown. An estimator is used as a parameter estimator to estimate the total control input, \hat{u} (Equation (3)). An estimate of u_{sig} is recovered by passing \hat{u} through a combination of notch and anti-notch filters. The filtered signature signal, \hat{u}'_{sig} , is defined as follows:

$$\hat{u}'_{sig}(z) = \frac{b_0 + b_1 z^1 + \dots + b_g z^g}{a_0 + a_1 z^1 + \dots + a_g z^g} \hat{u}(z) \quad (11)$$

where b_r, a_r for $r \in \{1, \dots, g\}$ represent the coefficients of the filter of order g . It is possible to recover \hat{u}'_{sig} because the perturbation signature has known frequency components that are passed through the series of filters. The synchronization of u_{sig} and \hat{u}'_{sig} is achieved by performing a correlation test, Equation (8), on both signals. As with the behavioral mode estimator, the current vehicle mode is determined using a metric to compare the error between \hat{u}'_{sig} and \tilde{u}^i_{sig} ,

$$\mathbf{v}^i(\mathbf{k}) = \begin{bmatrix} \hat{u}'_{sig}(k) - \tilde{u}^i_{sig}(k) \\ \vdots \\ \hat{u}'_{sig}(k-H) - \tilde{u}^i_{sig}(k-H) \end{bmatrix}. \quad (12)$$

III. PROBLEM STATEMENT

The proposed cooperative reconnaissance problem consists of assigning two unmanned aerial vehicles the task of searching an area containing $(M \times 2)$ target points. One of the vehicles is named the leader while the other is the follower. Initially, each vehicle is assigned a set of M target points. Each vehicle proceeds by flying to each target point, and circling the point with radius, R , until a level of information, I , is collected or a time constraint is met. A target point could be either an adversary, an obstacle, or be empty. Figure 4 shows a search area with three targets and the trajectory the leader would follow to collect information about Target 1.

Both vehicles are equipped with sensors that can locate and identify targets. However, each sensor has an associated uncertainty in location detection, such that it is beneficial to cooperate. One of the vehicles, the leader, flies over its assigned set of target points collecting information. If an adversarial target is detected, the leader notifies the second vehicle of the presence of the adversary by switching to the corresponding mode signature. As the vehicles traverse the target field, the follower monitors the movements of the leader. If a switch by the leader to a mode signaling the presence of an adversary is estimated, the follower evaluates a cost function in order to decide whether to leave its current target and fly to collect information about the leader’s target. Two metrics are used to evaluate switching. The first metric looks to minimize the time necessary to collect a certain degree of information. While the second metric, aims to maximize the amount of information collected in a fixed time interval. Once enough information is

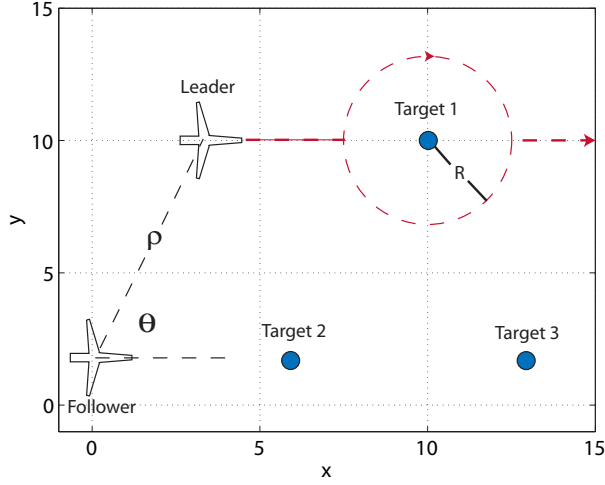


Fig. 4. Search area with three targets and the trajectory of the leader to collect information about Target 1. The radar measurements, ρ , θ are also shown.

collected or a time constraint is met, the follower returns to its previous target point.

A. System Model and Sensors

The vehicle dynamics are simplified by utilizing a linear point mass model to describe the motion in an inertial horizontal plane resulting in:

$$\dot{\mathbf{x}}(\mathbf{t}) = \begin{bmatrix} 0 & 1 & 0 & 0 \\ 0 & 0 & 0 & 0 \\ 0 & 0 & 1 & 0 \\ 0 & 0 & 0 & 0 \end{bmatrix} \mathbf{x}(\mathbf{t}) + \begin{bmatrix} 0 & 0 \\ 1 & 0 \\ 0 & 0 \\ 0 & 1 \end{bmatrix} \mathbf{u}(\mathbf{t}) + \mathbf{w}(\mathbf{t}), \quad (13)$$

where the state, $\mathbf{x}(\mathbf{t}) \in \mathbb{R}^4$, contains the position and velocity of the vehicle in the x and y directions, and $\mathbf{w}(\mathbf{t})$ is zero-mean Gaussian process noise with covariance Q . A zero-order hold with sampling T is used calculate the corresponding discrete model with state vector \mathbf{x}_k . Since the control inputs are unknown, they are estimated by augmenting the state to include these variables,

$$\mathbf{x}_k^a = \begin{bmatrix} \mathbf{x}_k \\ \mathbf{u}_k \end{bmatrix}. \quad (14)$$

Using full state feedback with gain K the bandwidth of the system is set to be 100 rad/sec.

The follower vehicle monitors the movements of the leader using radar measurements that provide data in polar coordinates: the range, ρ_k , and an angle, θ_k , relative to the heading of the follower, as shown in Figure 4. The nonlinear measurement equations are the following:

$$\begin{bmatrix} \rho_k \\ \theta_k \end{bmatrix} = \begin{bmatrix} \sqrt{(x_k^1 - y_k^1)^2 + (x_k^3 - y_k^3)^2} \\ \tan^{-1} \left(\frac{x_k^3 - y_k^3}{x_k^1 - y_k^1} \right) \end{bmatrix} + \mathbf{v}_k, \quad (15)$$

where x_k^i, y_k^i are the i th component of the leader and follower's state at time k and \mathbf{v}_k is zero-mean white Gaussian measurement noise with covariance R_v .

The behavior of the leader is described by three operating modes: flying/searching an empty target, adversary in target, obstacle in target. These modes are defined with the signatures shown in Table I.

TABLE I
OPERATING MODES AND CORRESPONDING MODE SIGNATURES.

Mode	Behavior	Signature
1	empty	[1 0 1 1 1 1 0]
2	enemy	[1 1 0 0 1 1 1]
3	obstacle	[0 1 1 1 0 1 1]

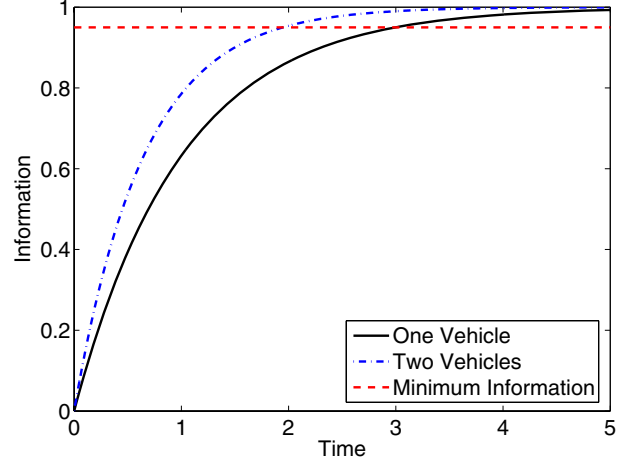


Fig. 5. Information curves when one and two vehicles collect information about a target. The dashed line represents the desired amount of information for the target.

B. Estimator

The mode estimation algorithm proposed in [6] requires an estimator to reconstruct the state of the leader. The nonlinear radar measurements proposed in this investigation require the use of a nonlinear estimator. It is well documented that the Sigma-point filter (SPF) is better able to deal with nonlinearities than the Extended Kalman Filter (EKF) [10], [11], [12]. It can be said that the EKF deals with nonlinearities with a first-order accuracy while the SPF achieves at least second-order accuracy [13]. Compared to the EKF, the SPF has similar computational complexity and does not require an analytic derivation of the Jacobian. For these reasons and for numerical stability, the square-root implementation of the SPF is chosen as the nonlinear estimator [14].

C. Information Collection and Cost

The objective of the vehicles is to collect information while circling around and sensing a target. In this investigation, the collection of information is modelled using an exponential function of the form:

$$I_i = I_0 \left(1 - e^{-\lambda_i t_i} \right), \quad (16)$$

where I_i is the information for the i th target, I_0 is constant, and λ_i is the information collection time constant. The value of λ_i is defined by the noise parameters, and whether one or two vehicles are collecting information about the i th target. The information curves, defined by Equation (16) for the case of collecting information with one ($\lambda = 1$) or two ($\lambda = 1.5$) vehicles respectively are shown in Figure 5. The advantage of collecting information cooperatively is shown as the information curve for the two vehicles has a steeper slope.

When the leader detects the presence of an adversary, the follower must decide whether collecting information cooperatively

will improve the mission objectives (information or time) through cooperation. A mission cost function is defined by: 1) maximizing the amount of information given a time constraint, or 2) minimizing the mission time given an amount of information is collected. The travel time between targets, $t^{i,j}$, and the information time constants are also part of the cost function.

Consider the case where the goal is to minimize the mission time given enough information is collected about each of the targets. The cost function is written as:

$$J_t = \min \sum_{i=1}^M t_i + \sum_{j=1}^M \sum_{l=1}^M t^{i,j}, \quad (17)$$

such that

$$I_0 \left(1 - e^{-\lambda_i t_i}\right) > I_{min}^i, \quad (18)$$

where t_i is the time spent collecting information (sensing) at the i^{th} target, $t^{i,j}$ is the travel time between the i^{th} and j^{th} target, and I_{min}^i is the desired amount of information for the i^{th} target. Once an adversary is detected, the follower evaluates Equation (17) with and without cooperation and changes its trajectory and signature appropriately.

In the case where the objective is to maximize the amount of information collected given a time constraint, the cost function is written as follows:

$$J_I = I_i \left(1 - e^{-\lambda_i t_i}\right) + \dots + I_M \left(1 - e^{-\lambda_M t_M}\right), \quad (19)$$

such that

$$T = \sum_{i=1}^M t_i + \sum_{j=1}^M \sum_{l=1}^M t^{i,j}. \quad (20)$$

By setting $\frac{\partial J_I}{\partial t_i} = 0$, the optimal value of t_i can be found analytically:

$$[t_1 \dots t_{M-1}]^T = (\lambda_N U + \text{diag}([\lambda_1 \dots \lambda_M]))^{-1} \begin{bmatrix} \ln \frac{I_1 \lambda_1}{I_M \lambda_M} + \lambda_M T \\ \vdots \\ \ln \frac{I_i \lambda_i}{I_M \lambda_M} + \lambda_M T \\ \lambda_M T \end{bmatrix}, \quad (21)$$

where $U \in \mathbb{R}^{M \times M}$ with elements all 1. If an adversary is detected by the leader, the follower evaluates Equation (19) with and without cooperation. In both Equations (17) and (19), cooperation is chosen unless either the cooperation time constant is not small enough and/or the distance between the follower and leader's target is too large.

IV. SIMULATION RESULTS

Two vehicles are assigned the task of searching a grid of (4 x 2) target points. There are four obstacles or adversaries randomly distributed between each row of the grid. The leader and follower vehicles start their trajectories at \mathbf{x}_0 and \mathbf{y}_0 respectively. Each vehicle collects information about a target by circling it with radius R . Depending on whether the target is identified as empty, an adversary, or an obstacle, different thresholds of information must be collected: I_{empty} , I_{enemy} , $I_{obstacle}$ respectively. The follower vehicle only flies to help the leader when the leader detects an adversary and the evaluated costs shows cooperation is useful. Monte Carlo simulations are used to gauge the performance of the vehicles. The simulation parameters used in the simulations are shown in Table II.

As a baseline, consider a fully decentralized strategy where each vehicle separately explores one side of the search area. In this scenario, there is no cooperation between the vehicles, thus

TABLE II
SIMULATION PARAMETERS FOR THE MONTE CARLO RUNS.

Parameter	Value
T	0.01
δ	0.10
ω	50 rad/sec
R	1
M	4
N	3
L	130
K	$\begin{bmatrix} 1.02 & 0.02 & -0.01 & 0 \\ -0.01 & 0 & 1.03 & 0.02 \end{bmatrix}$
I_{empty}	2000
I_{enemy}	4000
$I_{obstacle}$	3000
Q	$\text{diag}(0.01^2, 0.01^2, 0.01^2, 0.01^2, 0.01^2, 0.01^2)$
R_v	$\text{diag}(0.1^2, 0.05^2)$
λ_{single}	1
$\lambda_{cooperatively}$	1.6

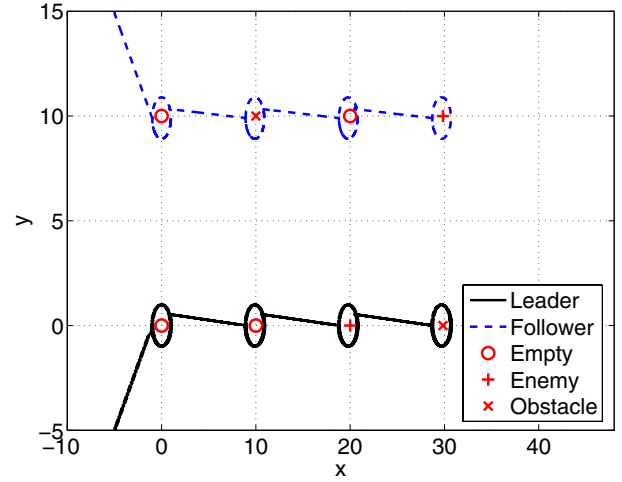


Fig. 6. Trajectories for the leader and follower when not cooperating.

no communication is required. The trajectories for the leader and follower are shown in Figure 6. A fully centralized solution is also simulated, where the leader immediately communicates for help whenever an adversary is detected. This strategy reduces the total time required to complete the mission because of the improved utility through cooperation (Figure 5). The trajectories for this strategy are shown in Figure 7. As shown in the figure, when the leader reaches its third target, the leader detects an adversary and communicates with the follower. The follower leaves its current target and circles the leader's third target. Once the information collected on the target is greater than the required threshold, the leader continues to its next target and the follower returns to the target it was tracking before the adversary was detected. For this configuration, when the vehicles fully communicate, the search time is 9% faster than the decentralized strategy.

When mode perturbation signatures are used, the vehicles exchange information without direct communication. However, there is an inherent delay in the follower's detection of the leader's mode because the information must pass through the dynamics of the nonlinear estimator, and the correlation test. To test the performance of the system, 25 simulations were conducted for the systems using a decentralized, centralized, and mode perturbation signature

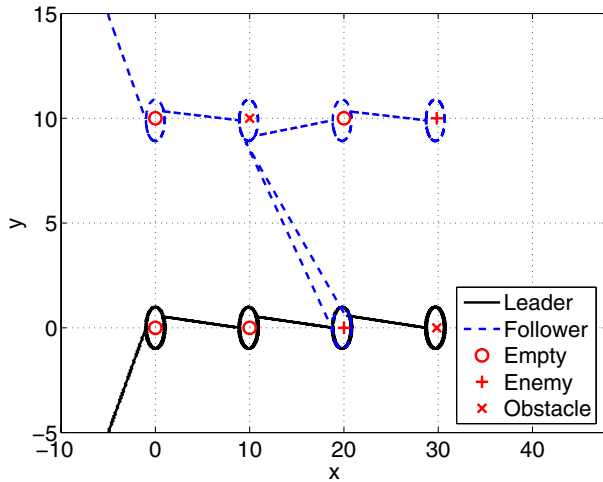


Fig. 7. Trajectories for the leader and follower with communication.

TABLE III
NORMALIZED TIME AVERAGE RESULTS.

Strategy	Average Normalized Time	Communication
Decentralized	1.00 ± 0.01	None
Centralized	0.86 ± 0.02	Full
Behavioral	0.92 ± 0.04	None
Filter based	0.90 ± 0.04	None

strategies (behavioral and filter based). The results shown in Table III are normalized by the time from the decentralized strategy. As shown in Table III, both mode estimation strategies are between the decentralized and centralized strategies. The performance results for the metric that measures the amount of information collected in a fixed time interval is shown in Table IV. The information is normalized by the information from the centralized strategy is emphasized that both mode estimation strategies search the area without direct communication.

The performance results for the two vehicles listed in Tables III and IV show that implementing mode perturbation signatures allow the vehicles to approach the performance of a centralized strategy without the use of direct communication (as in the decentralized strategy). The performance of the mode perturbation signature strategy is limited by various variables that include the distance between the leader and follower targets, and the information collection curves for the vehicles. These variables determine whether cooperation significantly improves performance. However, the simulations show that in certain cases mode perturbation signatures can effectively be used to transfer information between vehicles, thus allowing cooperation without the need of direct communication.

TABLE IV
NORMALIZED AVERAGE INFORMATION RESULTS.

Strategy	Average Normalized Information	Communication
Decentralized	0.82 ± 0.02	None
Centralized	1.00 ± 0.01	Full
Behavioral	0.89 ± 0.04	None
Filter based	0.88 ± 0.03	None

V. SUMMARY

A strategy using hybrid mode estimation has been developed and integrated into a cooperative reconnaissance problem in order to minimize communication between vehicles. The behavior of the leader was modelled as a hybrid system. Each node of the hybrid system was defined by the vehicle's dynamics as well as a mode perturbation signature. The cooperative performance of the system was defined by one of two metrics: 1) the length of time required by the two vehicles to collect a level of information, and 2) the total information collected in a fixed time interval. As the follower traverses the target field, it evaluates the performance metric to decide whether cooperation is beneficial. The results of Monte Carlo simulations showed that the performance of the system was better than the performance of a decentralized system with no cooperation, where both cases (time or information) required no communication. The performance was between the decentralized case (no cooperation and no communication) and the centralized case (with full communication and cooperation).

ACKNOWLEDGEMENTS

This work was supported by the Embedded & Hybrid Systems (EHS) program at the National Science Foundation.

REFERENCES

- [1] D. Weatherington, "Unmanned aerial vehicle (UAV) roadmap report," tech. rep., Department of Defense, 2003.
- [2] C. J. Tomlin, J. Lygeros, and S. S. Sastry, "A game theoretic approach to controller design for hybrid systems," *Proceedings of the IEEE*, 2000.
- [3] H. Blom and Y. Bar-Shalom, "The interacting multiple model algorithm for systems with markov switching coefficients," *IEEE Transactions on Automatic Control*, vol. 3, no. 8, pp. 780–783, 1988.
- [4] P. Otanez and M. Campbell, "Bounded model switching in uncertain hybrid systems," in *Proc. of the American Control Conference*, (Boston, MA), June 2004.
- [5] F. Ferrari-Trecate, D. Mignone, and M. Morari, "Moving horizon estimation for hybrid systems," *IEEE Transactions on Automatic Control*, vol. 47, pp. 1663–1676, October 2002.
- [6] P. Otanez and M. Campbell, "Mode estimation switching using perturbation signatures for hybrid multi-vehicle systems," in *Proc. of the AIAA Guidance, Navigation, and Control Conference*, August 2005.
- [7] R. Gold, "Optimal binary sequences for spread spectrum multiplexing," *IEEE Transactions on Information Theory*, vol. 13, no. 4, pp. 619–621, 1967.
- [8] R. L. Peterson, R. E. Ziemer, and D. E. Borth, *Introduction to Spread Spectrum Communications*. Prentice Hall, 1995.
- [9] Y. Bar-Shalom, X. R. Li, and T. Kirubarajan, *Estimation with Applications to Tracking and Navigation*. John Wiley and Sons, Inc., 2001.
- [10] S. Brunke and M. Campbell, "Estimation architecture for future autonomous vehicles," in *Proc. of the American Control Conference*, vol. 2, pp. 1108–1114, June 2002.
- [11] Y. Chen, T. Huang, and Y. Rui, "Parametric contour tracking using the unscented kalman filter," in *Proc. of the International Conference on Image Processing*, vol. 3, pp. 613–616, June 2002.
- [12] M. Andersen, R. Andersen, and K. Wheeler, "Filtering in hybrid dynamic bayesian networks," in *Proc. of the IEEE International Conference on Acoustics, Speech, and Signal Processing*, vol. 5, pp. 773–776, May 2002.
- [13] R. van der Merwe and E. Wan, "Sigma-point kalman filters for nonlinear estimation and sensor-fusion - applications to integrated navigation," in *Proc. of the AIAA Guidance, Navigation, and Control Conference*, August 2004.
- [14] S. Brunke and M. Campbell, "Square root sigma point filtering for real-time, nonlinear estimation," *Journal of Guidance, Control, and Dynamics*, vol. 27, no. 2, pp. 314–317, 2004.